Feedback cooling of levitated nanoparticles using the polarization of light

Muhammad Haider
King's College London
Supervised by Dr. James Millen & Dr. Maryam Nikkhou
(Dated: January 17, 2024)

Levitated nanorods exhibit rotational and translational motion when subjected to polarized light. Modulating the light intensity and degree of polarization ellipticity gives control over this motion. This has led to the development of ultra-stable driven nanomechanical devices, with applications in the precise measurement of forces at the quantum limit. This report will explore the theory behind levitated optomechanics, introducing an FPGA-based implementation of a feedback mechanism that leads to cooling of the rotational degrees-of-freedom of a levitated nanorod. A protocol is provided to produce the required result.

I. INTRODUCTION

The effects of laser light on dielectric particles were first reported by Arthur Ashkin in 1970 [1]. This was achieved by using a TEM_{00} mode beam of an argon laser focused through a solution of micro particles suspended within a liquid. It was shown that radiation pressure from the laser was able to impart a force on the particles along the direction of its propagation - the scattering force, $\mathbf{F}_{scat}$. Furthermore, particles with refractive index greater than the liquids were attracted to the lasers focus - through a gradient force, $\mathbf{F}_{grad}$. These principles were used by Ashkin and Dziedzic to realise the trapping (2D) of a 20 μm silica particle in free space [2] and later in a vacuum [3]. An electronic feedback system stabilising the particles centre-of-mass (c.o.m) motion was also introduced [4]. This utilised a novel linear feedback cooling mechanism, termed *cold damping*, which was able to cool a microparticle (R= 1.5 μm) to 1.5 mK.

In 2010, Li *et al.* were able to conduct linear feedback cooling on levitated microparticles in a high vacuum and showed that due to limits set by recoil heating (observing ballistic Brownian motion), smaller nanoparticles will have to be employed for cooling to the quantum regime [5, 6]. In 2012, a novel *parametric* feedback cooling mechanism developed by Gieseler *et al.* was able to cool the c.o.m motion of a levitated nanoparticle (R= 70 nm) to 50 mk [7]. This method used modulation of the laser intensity to change the stiffness of the trapping potential as a response to feedback of the c.o.m motion - working similarly to a damped harmonic oscillator. The rotational and torsional dynamics arising from trapped spherical nanoparticles have been studied in fluids [8, 9] and in free space [10, 11]. These types of interactions arise due to the transfer of *orbital* angular momentum from the lasers optical field to the levitated nanoparticle and offer applications in ultra precise measurement of forces at the quantum limit (as ground-state mechanical oscillators) [12–17]. This has been recently extended to include rotational control of cylinders and disks in a vacuum [18–20]. This is possible due to the transfer of *spin* angular momentum from the optical field. These dynamics were used to create an ultra-stable driven nanomechanical rotor that has torque sensitivities greater than 0.25 zNm [21].

The aim of this project is to show that an FPGA based device can be suitably used to control the feedback mechanism which leads to cooling of the rotational degrees-of-freedom (d.o.f) of a levitated nanorod.

II. EXPERIMENT

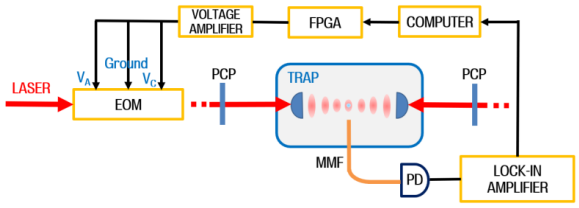

FIG. 1: Simplified view of the experiment schematic

A 1550 nm TEM_{00} laser is used to create an optical trap at the centre of a vacuum chamber. This is done by using a beam splitter to create two counterpropagating beams (acting as standing waves), with the trapping region in the centre. A silicon nanorod of diameter $d(= 130 \pm 13)$ nm and length $l(= 725 \pm 15)$ nm is trapped in the centre. A 1 mm core multi-mode fibre (MMF) placed close to the trap centre ($< 100\mu$m), collects scattered light from the trapped nanoparticle, yielding information about the translational and rotational degrees of freedom (d.o.f). This is connected to a photodetector (PD) which is able to convert the particles positional/ rotational data into an electrical signal. This data is then fed into a lock-in amplifier - a phase-locked-loop (PLL) that generates an output voltage with appropriate phase for parametric feedback cooling. The PLL being used is the Zurich Instruments HF2PLL [22]. Next the positional data and phase shift are recorded on a computer, before the voltage is transmitted to the FPGA. The FPGA performs some

fast data processing and and outputs two analog signals.

The outputs of the FPGA are in the form of two voltages; V_A and V_c. These voltages correspond to different settings of the electro-optic modulator (EOM) - which in turn controls settings on the polarization control paddle (PCP) to adjust the polarization of the incident laser beam. The PCP being used is from ThorLabs [23]. These PCP's incorporate a half-wave plate between two quarter-wave plates. By using this configuration, linear, circular and elliptical polarization states may be achieved. PCP's are placed at both directions of the trapping zone to control all incident laser polarization.

The values for V_A and V_C are calibrated by increasing the output PLL voltage, V, incrementally and measuring the corresponding polarization angle. This is seen for the half-wave plate in figure 11. These voltages are outputted into a voltage amplifier before being inputted the EOM. The EOM is also able to modulate the intensity of the trapping laser (through direct input of the PLL signal) to cool the translational motion of the trapped particle.

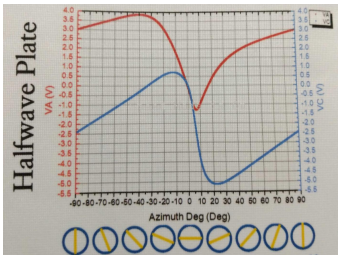

FIG. 2: Values of V_A and V_C calculated with a half-wave plate.

III. TRAPPING AND COOLING

Under the dipole approximation, a dielectric spherical nanoparticle of radius R$\ll \lambda$ (with λ being the wavelength of a TEM_{00} laser), experiences a force:

$$\langle \mathbf{F}_{\text{grad}} \rangle = \frac{\alpha'}{2} \langle \nabla \mathbf{E}^2 \rangle \tag{1}$$

where $\mathbf{E}$ is the complex electric field and $\alpha = \alpha' + \alpha''$ the complex polarizability. This *gradient* force traps the particle within the lasers focus (like a harmonic oscillator) and as such can be modelled as a restoring force:

$$\langle \mathrm{F}_{\text{grad},q} \rangle = -\mathrm{k}_q q \quad q \in \{x, y, z\} \tag{2}$$

where

$$k_{\mathrm{a}} = \frac{\alpha' E_0^2}{w_{a0}^2}, \quad k_{\mathrm{z}} = \frac{\alpha' E_0^2}{2 w_{z0}^2} \quad a \in \{x, y\} \tag{3}$$

is the trap stiffness, with w_{q0} being the beam waist. The equation of motion of the particle is given by:

$$\ddot{q}(t) + \Gamma_0 \dot{q}(t) + \Omega_0^2 q(t) = \frac{1}{m} F_{\text{fluct}}(t) \tag{4}$$

where m is the mass of the particle, $\Omega_0 = \sqrt{k_q/m}$ is the mechanical oscillation frequency, Γ_0 is the total momentum damping rate, F_{fluct} is the total fluctuating force that is defined through $\langle F_{\text{fluct}}(t) F_{\text{fluct}}(t') \rangle = 2m\Gamma_0 k_B T_0 \delta(t - t')$- a random Langevin encoding for a white-noise process. **Parametric feedback cooling** is possible by introducing a modulating force:

$$\ddot{q}(t) + \Gamma_0 \dot{q}(t) + \Omega_0^2 q(t) = \frac{1}{m} \left(F_{\text{fluct}}(t) + F_{fb}(t) \right) \tag{5}$$

where $F_{fb}(t)$=$k_{fb}(t)q(t)$ and $k_{fb}(t)$=$k_q \eta \sin(2\Omega_0 t + \phi)$ with ϕ being the relative phase of the particles motion to the trap frequency, η is the modulation depth, $\eta = I_{fb}/I_0$ with I_0 being the intensity of the laser before feedback and I_{fb} is the amplitude of the feedback modulation. By choosing ϕ that is $\pi/2$ out of phase with the particles motion, this becomes a damped harmonic oscillator and the particle's c.o.m motion is reduced.

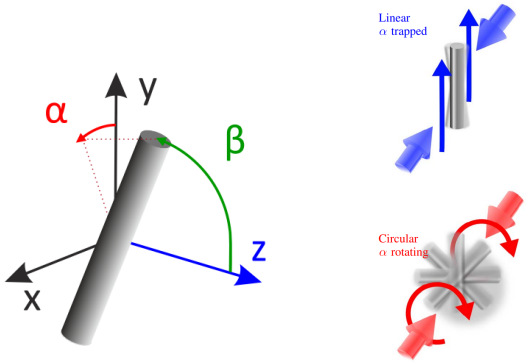

(a) a (b) b

FIG. 3: [a] Rotating cylinder. α is the angle between the x-axis and the projection onto the x-y plane. β is the angle between the cylinders symmetrical axis and the z-axis. From Ref. [24] [b] The two different types of rotations arising from linearly polarized light (top) and circularly polarized light (bottom). From Ref. [20]

When **linearly polarized** laser light is subject on a cylindrical particle with polarizability $\alpha_{\parallel}$ along the axial direction and $\alpha_{\perp}$ along the transverse direction, there is a nanoscale torque [25]:

$$\boldsymbol{\tau} = (\alpha_{\perp} - \alpha_{\parallel}) \left(E_y \hat{\mathbf{x}} - E_x \hat{\mathbf{j}} \right) E_z \tag{6}$$

that aligns the particles axis of symmetry along the polarization plane.

When **circularly polarized** laser light is subject on a cylindrical particle, there is a torque acting on α [20]:

$$N_\alpha = \frac{P_{\rm tot}\Delta\chi\ell^2 d^4 k^3}{48cw_0^2}\left[\Delta\chi\eta_1(k\ell)+\chi_\perp\eta_2(k\ell)\right] \quad (7)$$

where where d is the diameter of the cylinder, ℓ is the cylinders length, $\Delta\chi = (\varepsilon_{\rm r}-1)^2/(\varepsilon_{\rm r}+1)$ is the susceptibility anisotropy, $\chi_\perp$ is the susceptibility perpendicular to the rods symmetry axis and

$$\begin{aligned}\eta_1(k\ell) &= \tfrac{3}{4}\int_{-1}^{1} {\rm d}\xi\left(1-\xi^2\right){\rm sinc}^2\left(\tfrac{k\ell\xi}{2}\right)\\ \eta_2(k\ell) &= \tfrac{3}{8}\int_{-1}^{1} {\rm d}\xi\left(1-3\xi^2\right){\rm sinc}^2\left(\tfrac{k\ell\xi}{2}\right).\end{aligned} \quad (8)$$

The consequent PSD is found by measurement of the scattered light data [26]:

$${\rm PSD}(\Omega) = C_d^2\frac{2k_BT_0}{m_d}\frac{\Gamma_d}{\left(\Omega_d^2-\Omega^2\right)^2+\Omega^2\Gamma_d^2} \quad (9)$$

where d is the d.o.f (x,y,z,α,β), M_d is the particles mass (x,y,z) or the moment of inertia (α,β), Ω_d is the trapping frequency, Γ_d is the angular momentum damping rate, T_0 is the c.o.m temperature and C_d is the calibration between the measured signal and the actual motion of the nanoparticle. By applying parametric feedback on all d.o.f, the modulating feedback results in a slight shift in the total momentum damping rate by $\delta\Gamma$ and the mechanical oscillation frequency by $\delta\Omega$. The PSD becomes:

$$PSD(\Omega) = C_d^2\frac{\Gamma_d k_B T_0/(\pi m)}{\left(\left[\Omega_d+\delta\Omega\right]^2-\Omega^2\right)^2+\Omega^2\left[\Gamma_d+\delta\Gamma\right]^2} \quad (10)$$

By integrating both sides over Ω, the mean square displacement is found:

$$\begin{aligned}\left\langle q^2\right\rangle &= \int_0^\infty PSD(\omega)d\omega\\ &= \frac{\Gamma_d k_b T_0}{m}\frac{1}{\omega_0^2\left(\Gamma_d+\delta\Gamma\right)}\end{aligned} \quad (11)$$

Through the equipartition theorem, $k_BT_{\rm eff} = m\left(\Omega_d+\delta\Omega\right)^2\left\langle q^2\right\rangle$. For the limit $\delta\Omega \ll \Omega_d$, the effective c.o.m temperature becomes:

$$T_{\rm eff} = T_0\frac{\Gamma_0}{\Gamma_0+\delta\Gamma} \quad (12)$$

where T_0 is the c.o.m temperature in the absence of parametric feedback cooling. Thus it is seen that temperature may be raised or lowered, depending on the sign of $\delta\Gamma$.

Feedback cooling procedure:

Translational parametric feedback cooling is achieved by modulating the intensity of the trapping laser. The outputted PLL signal is sent directly to the EOM, which is able to control the trapping lasers intensity and cool the translational d.o.f (x,y,z) of the trapped nanorod's c.o.m motion.

Polarisation parametric feedback cooling is achieved by using the FPGA's outputted V_A and V_C voltage signals. When the laser is circularly polarized, the interaction between scattered light produces a torque that forces the particle in the plane orthogonal to the beam axis, while it's c.o.m motion remains trapped due to translational feedback cooling. The polarization response cools the rotational d.o.f (α and β).

IV. FPGA IMPLEMENTATION

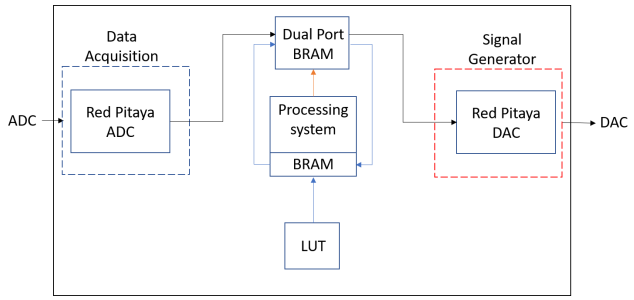

FIG. 4: Simplified Block Diagram of the FPGA implementation

The FPGA being used is *STEMlabs* Red Pitaya (RP). Programming is primarily achieved within the Xilinx Vivado software environment.The PLL output signal, V, is inputted through one of the RP's 14 bit ADC channels. A *Data Acquisition* hierarchy, housing a RP ADC module receives the data and sends it to an input on the Dual Port BRAM module. This is achieved through an AXI stream protocol and is able to interface with the processing system through an AXI interconnect (not shown in simplified diagram) [27]. The *LUT* hierarchy instantiates the pre-calibrated values of V, V_A and V_C into the BRAM. The *Dual Port BRAM module* takes the inputted V signal and finds the corresponding V_A and V_C values within the BRAM. This is sent to the *Signal Generator* hierarchy which houses a RP DAC module - that is able to output the data directly to the two RP 14 bit DAC channels. The LUT may be instantiated into the BRAM by using Xilinx's Data2MEM tool [28].

V. EXPECTED RESULTS AND ANALYSIS

Unfortunately, programming of the Red Pitaya could not be completed to obtain any meaningful results. In particular, there were difficulties with instantiating the LUT in the BRAM. A protocol has been provided to produce two of the main components within the project file. Had the project been successful, the output would have been the production of output signals corresponding to the V_A and V_C output voltages. Following the Vivado project flow, a simulation test bench could have been run and an analysis (see [29]) on the results conducted. The main source of error in this project is the RP high input noise ($\sim 1\frac{\mu V}{\sqrt{Hz}}$ [30]). This is especially high when compared with the input noise of the PLL ($5\frac{nV}{\sqrt{Hz}}$ [22]). There are also some latency errors arising from the ADC (48 ns [31]) and DAC (43 ns [32]). Although these are considered insignificant as the system is running at $\sim 10MHz$ ($\sim 1 \times 10^{-6}s$). However it should be noted that these processing latencies may lead to group delay between the input and output signals. The consequent phase response may develop linear frequency dependencies which limits the effective bandwidth of the feedback system. For a group delay of τ_g=91 ns, there is a frequency dependent phase response [33]:

$$\frac{\mathrm{d}\phi}{\mathrm{d}\nu} = -\tau_g 360 \approx \frac{33^\circ}{\mathrm{MHz}} \tag{13}$$

Errors from other sources must also be considered. The electrical noise floor can be lowered by changing the PLL amplifier with a lower noise version. Doing so will allow the feedback mechanism to reach lower c.o.m temperatures (as PSD will have greater resolution). Another way to decrease electrical noise is by increasing the signal to noise ratio (SNR), this can be achieved by placing a low noise voltage amplifier after the detector [34]. As a consequence of all inherent equipment noise, the RP's feedback scheme may create a positive feedback loop such that the feedback signal grows without bound until the RP's output limit has been reached. This is referred to as *parasitic feedback* and has been documented before in feedback cooling [35].

[1] A. Ashkin 10.1103/PhysRevLett.24.156 (1970).
[2] A. Ashkin and J. M. Dziedzic 10.1063/1.1655064 (1974).
[3] A. Ashkin and J. M. Dziedzic 10.1063/1.88748 (1976).
[4] A. Ashkin and J. M. Dziedzic 10.1063/1.89335 (1977).
[5] T. Li *et al.* 10.1126/science.1189403 (2010).
[6] T. Li *et al.* 10.1038/nphys1952 (2011).
[7] J. Gieseler, *Dynamics of optically levitated nanoparticles in high vacuum*, Ph.D. thesis, The Institute of Photonic Sciences (2014).
[8] A. L. Porta and M. Wang 10.1103/PhysRevLett.92.190801 (2004).
[9] A. I. Bishop *et al.* 10.1103/PhysRevLett.92.198104 (2004).
[10] M. Bhattacharya *et al.* 10.1103/PhysRevLett.99.153603 (2007).
[11] Y. Arita *et al.* 10.1038/ncomms3374 (2013).
[12] J. Chan *et al.* 10.1038/nature10461 (2011).
[13] A. D. O'Connell *et al.* 10.1038/nature08967 (2010).
[14] P. F. Barker 10.1103/PhysRevLett.105.073002 (2010).
[15] S. Gröblacher *et al.* 10.1038/nphys1301 (2009).
[16] I. Wilson-Rae *et al.* 10.1103/PhysRevLett.99.093901 (2007).
[17] G. Ranjit *et al.* 10.1103/PhysRevA.93.053801 (2016).
[18] S. Kuhn *et al.* 10.1021/acs.nanolett.5b02302 (2015).
[19] B. A. Stickler *et al.* 10.1103/PhysRevA.94.033818 (2016).
[20] S. Kuhn *et al.* 10.1364/optica.4.000356 (2017).
[21] S. Kuhn *et al.* 10.1038/s41467-017-01902-9 (2017).
[22] Z. Instruments, Hf2pll phase-locked loop leaflet, `https://www.zhinst.com/sites/default/files/documents/2020-01/zi_hf2pll_leaflet_0.pdf` (2018), [Online; accessed 08/04/2021].
[23] ThorLabs, Manual fiber polarization controllers, `https://www.thorlabs.com/newgrouppage9.cfm?objectgroup_id=343` (2018), [Online; accessed 08/04/2021].
[24] J. Millen *et al.* 10.1088/1361-6633/ab6100 (2020).
[25] D. S. Bradshaw and D. L. Andrews 10.1088/1361-6404/aa6050 (2017).
[26] S. Kuhn *et al.* 10.1364/OPTICA.4.000356.s001 (2017).
[27] XILINX, Axi reference guide, `https://www.xilinx.com/support/documentation/ip_documentation/axi_ref_guide/v13_4/ug761_axi_reference_guide.pdf` (2012), [Online; accessed 08/04/2021].
[28] XILINX, Data2mem user guide, `https://www.xilinx.com/support/documentation/sw_manuals/xilinx11/data2mem.pdf` (2009), [Online; accessed 08/04/2021].
[29] XILINX, Logic simulation, `https://www.xilinx.com/support/documentation/sw_manuals/xilinx2016_1/ug937-vivado-design-suite-simulation-tutorial.pdf` (2016), [Online; accessed 08/04/2021].
[30] S. R. Pitaya, I/o specifications, `https://redpitaya.readthedocs.io/en/latest/developerGuide/125-14/fastIO.html#` (2021), [Online; accessed 08/04/2021].
[31] L.-. Datasheet, Analog devices, `https://www.analog.com/media/en/technical-documentation/data-sheets/21454314fa.pd` (2017), [Online; accessed 08/04/2021].
[32] D. Datasheet, Integrated device technology, `https://www.renesas.com/eu/en/document/dst/dac1401d125-datasheet` (2012), [Online; accessed 08/04/2021].
[33] J. Herkenhoff, Development of a digital feedback system for advanced ion manipulation techniques within a penning trap (2020).
[34] J. Vovrosh, *Parametric feedback cooling and squeezing of optically levitated particles*, Ph.D. thesis, University of Southampton (2018).
[35] J. Nätkinniemi, *Optical feedback cooling of a mechanical silicon oscillator with a single laser*, Master's thesis, Department of Physics University of Jyväskylän (2020).